Dynamics and electronic properties of the Tl^+-perturbed $Tl^0(1)$ center in KCl, KBr, and RbCl as probed by resonant Raman scattering

Wim Joosen, Etienne Goovaerts, and Dirk Schoemaker
Department of Physics, University of Antwerp, B-2610 Wilrijk (Antwerp), Belgium
(Received 27 October 1986)

Inelastic light scattering of the Tl^+-perturbed $Tl^0(1)$ center [denoted as $Tl^+Tl^0(1)$] in KCl, KBr, and RbCl is resonantly excited in its two visible optical transitions. The absorption spectrum of $Tl^+Tl^0(1)$ shows some similarities with that of the laser-active $Tl^0(1)$. The Raman spectra obtained under excitation of the third optical band of $Tl^+Tl^0(1)$ contrast with those of $Tl^0(1)$ under "*F*-like" excitation by the spectral composition of the defect-induced first-order spectrum, and by the absence of a low-frequency $Tl^0(1)$-like mode at about 30 cm^{-1}. A behavior-type (BT) analysis of the polarized Raman intensities establishes an apparent C_{4v} symmetry. The selective resonant enhancement of one diagonal component of the Raman tensor under excitation of the third optical transition of $Tl^+Tl^0(1)$ obscures the low defect symmetry. The latter shows up in the polarized Raman spectra obtained under excitation of the fourth optical band. These spectra do exhibit a low-frequency mode at about 25 cm^{-1}, which is associated with the motion of one or both of the thallium nuclei. The analysis of this mode by means of the extended BT method for resonant Raman scattering establishes that it belongs to the totally symmetric representation of either the $C_{1h}[010]$ or the $C_{2v}[110]$ point group. The former defect symmetry corresponds to a weakly perturbed $Tl^0(1)$ center, while the latter is compatible with electron tunneling between two equivalent thallium nuclei.

I. INTRODUCTION

The study of the laser-active color centers in alkali halides has been of continued interest during the last two decades. Several types of potential laser defects are reviewed in Ref. 1. For the present paper laser centers of the atomic type will mainly be of interest, which, in contrast with the so-called F_A(II) and F_B(II) centers, involve an almost completely reduced cation of high electron affinity and an adjacent anion vacancy. The prototype of the latter defects is the $Tl^0(1)$ center in KCl, which was discovered and extensively studied by means of conventional electron spin resonance (ESR).[2,3] Reliable laser performance of $Tl^0(1)$ was achieved in KCl and KBr host crystals.[4,5] Subsequently, a large amount of similar defects possessing the so-called "laser-active-type structure" in alkali halides with ns^2 ions (Ga^+, In^+, Sn^{2+}, Pb^{2+}) have been studied by ESR and optical absorption, and relevant literature is listed in Ref. 6.

A model of the $Tl^0(1)$ center, in which a thallium atom is positioned in an axial crystal field, was shown to explain the peak positions and the polarization properties of the three lowest-energy optical transitions.[7] Optical bands of higher energy probably associated with the excitations to more delocalized continuumlike states have also been reported, but these transitions were not investigated within the framework of the atomic thallium model.[7,8] Another experimental identification of the $Tl^0(1)$ absorption bands was provided by measurements of their magnetic circular dichroism (MCD) tagged to the ESR transitions and by optical detection of magnetic resonance (ODMR).[8] This study of $Tl^0(1)$ also yielded the discovery of a new thallium aggregate center.

Very recently, the latter center was studied by ODMR and MCD measurements in KCl, RbCl, and KBr.[9] It was shown to consist of two adjacent substitutional Tl^+ ions around an anion vacancy, exchanging one unpaired electron. According to some of its polarized Raman properties, we prefer to consider the new thallium dimer center as a Tl^+-perturbed $Tl^0(1)$ center and adopted the notation $Tl^+Tl^0(1)$.[9] The MCD spectra of this center show some similarities with those of $Tl^0(1)$: the three lowest optical transitions (OT) of $Tl^+Tl^0(1)$ in KCl peak at 1070, 800, and 635 nm.[10] We shall call these optical transitions OT1, OT2, and OT3, in that order. They are tentatively associated with the $Tl^0(1)$ transitions at 1060, 725, and 550 nm, respectively.[7,8] However, differences in polarization properties may be expected, since the [100] direction is no longer a symmetry axis of the dimer center.[9]

Knowledge about the absorption bands of $Tl^0(1)$ and $Tl^+Tl^0(1)$ offers interesting perspectives for resonant Raman scattering (RRS). Inelastic light scattering of $Tl^0(1)$ in several alkali halides have been resonantly excited in its OT3, i.e., the so-called "*F*-like" band.[10] The latter is associated with the transition between the $6P_{1/2}$ ground level and the $7S_{1/2}$ level of the free thallium atom,[7,8] and peaks near to the maximum of the *F* band.[11] The $Tl^0(1)$ Raman spectrum consists of a low-frequency resonance at about 30 cm^{-1}, which reflects the motion of the thallium atom along the fourfold axis of the C_{4v} symmetry, and an induced first-order spectrum, which is associated with breathing modes of the surrounding chloride ions. Preliminary results on the Raman spectra of $Tl^+Tl^0(1)$ were also reported in Ref. 10.

In the present work resonant Raman measurements are reported for the $Tl^+Tl^0(1)$ center under excitation of its

OT3 and OT4 (Refs. 8 and 9). It will be shown that the observed behavior type[12] (BT) of the polarized Raman spectra under OT3 excitation directly points to a C_{4v} symmetry, which was also established for the unperturbed $Tl^0(1)$ center.[2,10] Surprisingly, no low-frequency dynamical mode at about 30 cm^{-1} was observed. Therefore, polarized Raman experiments with excitation in OT4 of $Tl^+Tl^0(1)$ have also been performed. The resulting Raman spectra exhibit a low-frequency mode associated with the motion of one or two thallium nuclei. This resonance has been analyzed within the framework of the extended BT method for RRS of randomly oriented centers in cubic crystals,[13] and this analysis provides evidence of the lower symmetry of the dimer center with respect to the unperturbed $Tl^0(1)$ defect.

Section II deals with some experimental details. In Sec. III the essential features of the $Tl^+Tl^0(1)$ spectra are summarized. Section IV contains the BT analysis of the polarized Raman data. In Sec. V two alternative viewpoints will be considered in order to explain the polarized Raman data: The resonant Raman technique may, possibly depending on the laser frequency, probe either an electron that is equally distributed over two equivalent thallium sites, i.e., an electron tunneling system, or an electron on only one thallium nucleus, i.e., a perturbed $Tl^0(1)$ center.

II. EXPERIMENTAL PROCEDURES

The samples used in this investigation were grown from melts containing typically 2 mol% of the appropriate thallium halide. The crystals were x-ray irradiated for 90 min at 250 K, and subsequently, they were F bleached using a halogen lamp and a suitable interference filter for about 5 min at the same temperature. After this procedure, sizable amounts of both $Tl^0(1)$ and $Tl^+Tl^0(1)$ defects were detected, while the remaining F-center concentration was negligible. The production was monitored by parallel optical-absorption and Raman measurements (see Sec. III). All the data were recorded at 10 K.

The Raman spectra under OT3 excitation were obtained by means of a Kr^+ laser (Spectra Physics Model No. 2025-11) and a 4-mW He-Ne laser. The OT4 were excited with an Ar^+ laser (Spectra Physics Model No. 165). In particular, the 514.5-nm line was used for KBr:Tl^+ and RbCl:Tl^+, while the line at 457.9 nm was suitable for KCl:Tl^+. In order to minimize bleaching effects, the lasers were operated at moderate powers below 50 mW. Details about the Raman equipment are presented in Ref. 14.

III. IDENTIFICATION OF THE RAMAN SPECTRA

A. Correlation with optical absorption and MCD measurements

The production process described in Sec. II yields considerable amounts of $Tl^0(1)$ defects and $Tl^+Tl^0(1)$ dimer centers. In Fig. 1 the relevant optical transitions OT3 and OT4 in RbCl:Tl^+ and KBr:Tl^+ are presented for different time intervals of F bleaching. *Optical-absorption* measurements show that it is impossible to produce $Tl^+Tl^0(1)$ without sizable amounts of $Tl^0(1)$. However, a suitable

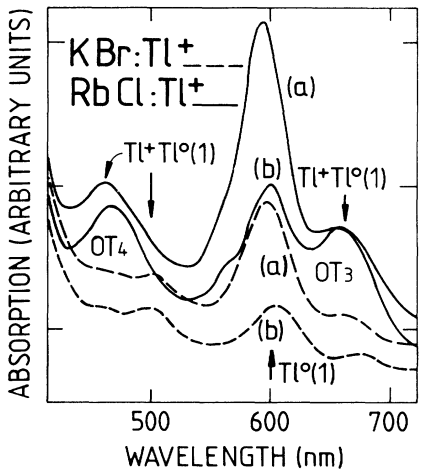

FIG. 1. Optical-absorption spectra of KBr:Tl^+ (dashed lines, 1.7 mol% of TlBr in the melt) and RbCl:Tl^+ (solid lines, 0.3 mol% of TlCl in the melt). The spectral regions of $Tl^+Tl^0(1)$ absorption are indicated by arrows. (a) After 45 min of F bleaching at low T; (b) after another 2 min of F bleaching at 250 K.

time of exposure to F light enhances the relative concentration of the dimer center, and this allows one to isolate the $Tl^+Tl^0(1)$ *Raman* spectra from that of $Tl^0(1)$.

Parallel to the absorption measurements, the Raman spectra under OT3 excitation were recorded. A superposition of $Tl^0(1)$ and $Tl^+Tl^0(1)$ spectra was observed and some of these composite Raman spectra have been reported earlier.[10] A peculiarity, which is very useful for the identification of the dimer spectra, is that the low-frequency Raman mode, which is characteristic for the $Tl^0(1)$ center, disappears for higher relative concentrations of the dimer center. As a result, the dimer spectrum can be isolated from the $Tl^0(1)$ spectrum. This is illustrated for RbCl:Tl^+ in Figs. 1 and 2. The same phenomenon

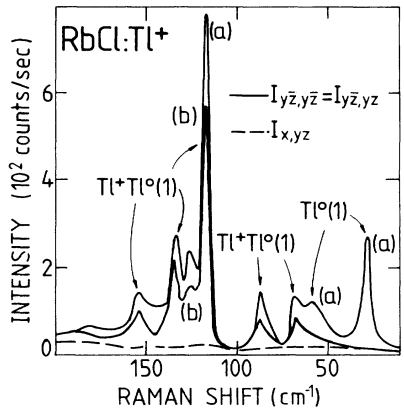

FIG. 2. Polarized Raman spectra of RbCl:Tl^+ under 632.8-nm excitation (4 mW), measured parallel with the optical-absorption data of Fig. 1. The low-frequency mode of $Tl^0(1)$ and its first overtone are still observable after 45 min of F bleaching at low T (curve a), but disappear upon another 2 min of F bleaching at 250 K (curve b). The I_{yz} intensities of $Tl^0(1)$ and $Tl^+Tl^0(1)$ are zero (dashed line).

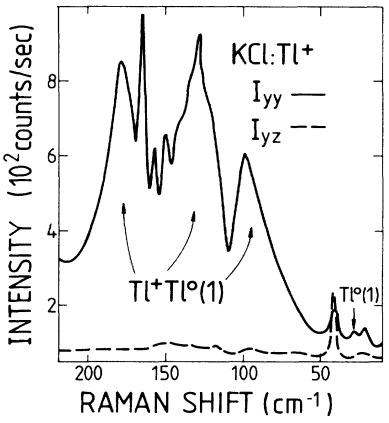

FIG. 3. Polarized Raman spectra of $Tl^+Tl^0(1)$ in KCl:Tl^+ (1.9 mol % of TlCl in the melt), under excitation at 647.1 nm (50 mW). The localized mode at (43 ± 1) cm^{-1}, which clearly shows up in the I_{yz} spectrum, does not belong to $Tl^+Tl^0(1)$.

was established in KCl:Tl^+ and KBr:Tl^+ (see Figs. 3 and 4). This observation strongly supports the identification of the $Tl^+Tl^0(1)$ spectra under OT3 excitation.

It should be mentioned that the absorption spectra of KCl:Tl^+ are not presented here, since the MCD data for $Tl^0(1)$ and $Tl^+Tl^0(1)$ in KCl are explicitly given in Refs. 8 and 9, respectively.

B. Correlation between Raman spectra for different excitation frequencies

Under 514.5 and 457.9-nm excitation, the Raman spectra of $Tl^+Tl^0(1)$ could not be completely isolated from the spectral contributions of other thallium aggregate centers. The main reason for this is the possible overlap in the spectral region of interest of several optical transitions with rather small oscillator strengths and belonging to different centers. Only for KCl:Tl^+ has the MCD spectrum of $Tl^+Tl^0(1)$ in this region been reported:[8,9] The signal maximum is centered at 450 nm and secondary maxima

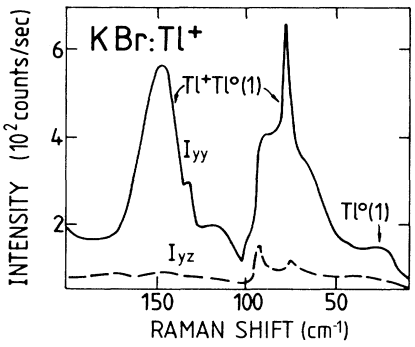

FIG. 4. Polarized Raman spectra of $Tl^+Tl^0(1)$ in KBr:Tl^+ (1.7 mol % of TlBr in the melt) under 676.4-nm excitation (45 mW). The strongest peak in the I_{yz} spectrum does not belong to $Tl^+Tl^0(1)$.

show up in its low- and high-frequency tails. For KBr:Tl^+ and RbCl:Tl^+, no MCD spectra have been published, making it necessary for us to perform conventional optical-absorption experiments. This technique, however, does not allow one to unravel the different contributions to the absorption signal, as is possible by the tagged MCD measurements. Nevertheless, we associated the absorption bands at about 480 nm in KBr:Tl^+ and RbCl:Tl^+ (Fig. 1) with the OT4 of $Tl^+Tl^0(1)$ in KBr and RbCl. In making this correspondence, we considered that probably also for $Tl^+Tl^0(1)$, a larger lattice constant parallels a shift of the absorption maxima to smaller frequencies, as was established for $Tl^0(1)$ in several alkali halides.[11]

The Raman modes obtained under 457.9-nm excitation in KCl:Tl^+ and under 514.5-nm excitation in KBr:Tl^+ and RbCl:Tl^+ will be reported and analyzed below. They are associated with the $Tl^+Tl^0(1)$ center on the basis of the following results.

(i) Similar production processes as in Refs. 2 and 9 have been used. Raman modes of other thallium aggregate centers could be recognized, first because of their changing relative intensities with respect to the intensity of the $Tl^+Tl^0(1)$ modes, which are very sensitive to both the details of the production process and the frequency of the exciting laser line, and second because they often possess different polarization properties (see, e.g., Figs. 3 and 4).

(ii) The production of $Tl^0(1)$ and $Tl^+Tl^0(1)$ was monitored in optical absorption, and a correlation was established with the Raman intensity under appropriate excitation of the OT3 of $Tl^+Tl^0(1)$.

(iii) After isolation of the $Tl^+Tl^0(1)$ Raman spectrum (Sec. III A), parallel resonant Raman experiments were performed under 514.5- and 457.9-nm excitation, and correlation has been established between the spectral features in these Raman data and those obtained under OT3 excitation. However, this correspondence is comparatively more clear in KBr and RbCl, than in KCl.

(iv) The polarized Raman intensities of the $Tl^+Tl^0(1)$ modes are consistent with the $C_{2v}[110]$ symmetry which was established with the optically detected ESR (ODESR) and MCD techniques. This will be discussed in Sec. IV.

(v) The fact that similar general characteristics concerning the polarized Raman intensities and the spectral composition have been observed in the three alkali halides under study provides an additional argument for the validity of our identification.

The spectral features belonging to other thallium aggregate centers, which appear in the presented Raman spectra, are explicitly indicated in the figure captions.

C. Characteristics of the Tl^+-perturbed $Tl^0(1)$ Raman spectra

The polarization characteristics and the spectral composition of the Raman spectra of $Tl^+Tl^0(1)$ depend on the excitation frequency in a peculiar way. Some representative polarized Raman spectra under OT3 excitation are presented in Figs. 2, 3, and 4. In all the crystals under study, a first-order phonon spectrum is induced by the

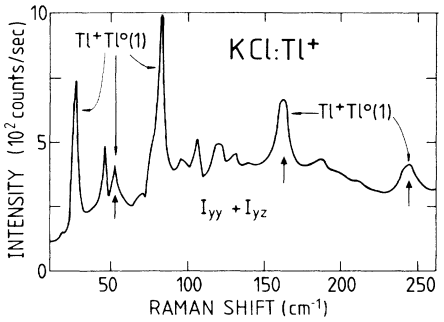

FIG. 5. Unpolarized Raman spectrum of KCl:Tl^+ (1.9 mol % of TlCl in the melt) after x-ray irradiation at RT, under 457.9-nm excitation (2 mW). The overtones of the 26-cm^{-1} and the 81-cm^{-1} modes of $Tl^+Tl^0(1)$ are indicated by small vertical arrows. The unidentified mode at 43 cm^{-1} (see Fig. 3) reappears in this spectrum.

$Tl^+Tl^0(1)$ center. No low-frequency vibrations around 30 cm^{-1} are observed. Stated otherwise, the motion of the thallium atom along the C_{4v} defect axis, which dominantly contributes to the $Tl^0(1)$ spectrum under "*F*-band" excitation, does not show up in the dimer spectrum, when the latter is resonantly excited in OT3.

When the Raman scattering of $Tl^+Tl^0(1)$ is excited in its OT4 a low-frequency mode is detected, peaking at 26 cm^{-1} in KCl and at 22 cm^{-1} in RbCl and KBr (Figs. 5, 6, and 7). Some resonances which are observed under OT3 excitation reappear in this spectrum. A summary of the most prominent spectral features of $Tl^+Tl^0(1)$ is given in Table I. The polarized Raman intensities are discussed in detail in the next section, for the particular case of RbCl:Tl^+.

IV. BEHAVIOR-TYPE ANALYSIS OF THE POLARIZED RAMAN DATA UNDER RESONANT EXCITATION IN VARIOUS OPTICAL BANDS

A. Behavior-type method for nonresonant scattering

The BT method was developed to analyze the polarized Raman intensities of dynamical modes of point defects in

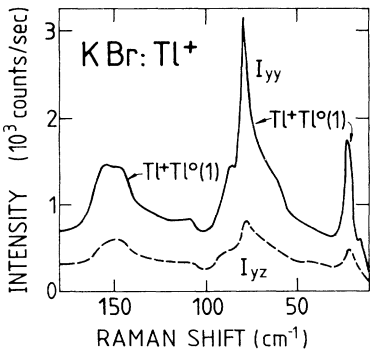

FIG. 6. Polarized Raman spectra of $Tl^+Tl^0(1)$ in KBr:Tl^+ (1.7 mol % of TlBr in the melt) after x-ray irradiation at RT, under 514.5-nm excitation (40 mW).

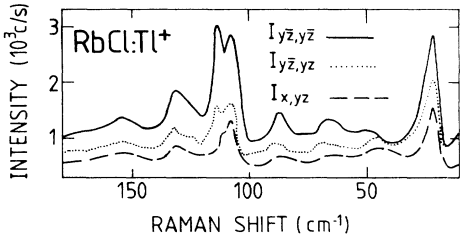

FIG. 7. Complete set of polarized Raman data of $Tl^+Tl^0(1)$ in RbCl:Tl^+ (see Fig. 2) under 514.5-nm excitation (100 mW). The spectra have been corrected for bleaching effects, which are due to the resonant laser light.

cubic crystals. It allows one to determine the irreducible representation of the observed Raman mode and the local point group of the defect within clearly spelled-out limits. First, only symmetric Raman tensors have been considered, yielding a method which initially was meant to apply to nonresonant Raman scattering only.[12] The usefulness of this BT approach has been demonstrated for several perturbed interstitial hydrogen-atom centers in alkali halides.[14,15] Subsequently, it allowed us to determine the nature of the low-frequency resonance of the Li^+ off-center ion in KCl.[16]

The polarized Raman study of the laser-active $Tl^0(1)$ center under resonant excitation of its *F*-like band,[10] necessitated a reappraisal of the BT method for the case of RRS. However, it was experimentally shown that the off-diagonal components of the Raman tensor are all equal to zero. As a result, the original BT approach remained fully applicable. The same situation occurs for the polarized Raman data of $Tl^+Tl^0(1)$ under OT3 excitation, as will be briefly discussed in Sec. IV C.

B. Behavior-type analysis for resonant Raman scattering

The Tl^+-perturbed $Tl^0(1)$ center, as well as the $F_A(Li^+)$ center in KCl,[13] possess Raman modes with a nonzero depolarized scattering under resonant excitation in some of their optical transitions. A proper analysis of the polarized Raman data of such modes necessitates a substantial extension of the original BT method. In a joint effort with Leblans, we studied the modifications of the BT method for RRS. Some crucial aspects of this extended theory, which will be denoted by RRS BT, are discussed in the Appendix of Ref. 13.

The RRS BT method will be applied to the low-frequency resonance of $Tl^+Tl^0(1)$ in RbCl:Tl^+, which is observed under OT4 excitation. This particular Raman mode is representative for the $Tl^+Tl^0(1)$ resonances in the three host crystals under study. The conclusion of this RRS BT analysis will be combined with the results of the *original* BT method, which still applies to the polarized Raman data under excitation of OT3. In the next two subsections it will be demonstrated that this *combined* BT approach[13] yields more precise information about the symmetry of the $Tl^+Tl^0(1)$ dimer center.

TABLE I. The vibrational energy ω (in cm^{-1}) of the most prominent Raman resonances of the $Tl^+Tl^0(1)$ center, as well as the number of their observable overtones n, are listed for three alkali halides. The wavelength (in nm) of the exciting laser light λ_L is compared to the maximum λ_m of the absorption bands of the Tl^+-perturbed $Tl^0(1)$ center.

Crystal	λ_m[a] (nm)	λ_L (nm)	$\omega[Tl^+Tl^0(1)]$ (cm^{-1})	n[b]
KCl	635	632.8, 647.1	c	c
	450	457.9	26	1
			81	3
RbCl	665	632.8, 647.1	117	2
	480	514.5	22	1
			112	0
KBr	675	676.4, 647.1	78	0
	480	514.5	22	1
			78	0

[a]See Sec. III A and Refs. 7–9.

[b]This number is very sensitive to the frequency of the excitation light; the reported number n is not always directly connected with the presented Raman spectra.

[c]In comparison with KBr:Tl^+ and RbCl:Tl^+, there are no Raman resonances of outstanding intensity in KCl:Tl^+ under OT3 excitation.

C. Apparent C_{4v} symmetry under excitation in the third optical band of $Tl^+Tl^0(1)$

As a representative case, the $Tl^+Tl^0(1)$ center in RbCl is considered. It is shown in Fig. 2 that the *relative* Raman intensities of $Tl^0(1)$ for different polarization geometries are equal to the corresponding ones of $Tl^+Tl^0(1)$ under excitation of their respective OT3. Therefore, we will not present a detailed outline of the BT analysis of these polarized Raman data. The same arguments, which are formulated in Sec. IV A of Ref. 10, apply to this case.

It is concluded that the polarized Raman intensities of $Tl^+Tl^0(1)$ under OT3 excitation possess an observed BT, which directly points to an A_1 mode in a C_{4v} defect symmetry. This result may suggest that $Tl^+Tl^0(1)$ is a weakly perturbed $Tl^0(1)$ center, since the Raman scattering does not detect the lower symmetry, caused by the presence of the additional Tl^+ ion. However, the combined BT approach given in Sec. IV D, which also takes into account the Raman data under OT4 excitation, will demonstrate that this conclusion is too hasty.

D. Evidence for the lower symmetry of $Tl^+Tl^0(1)$

It will be shown that the polarized Raman data of RbCl:Tl^+, obtained under 514.5-nm excitation, yield an observed BT $D_2[110]:A$, which points to the low symmetry of $Tl^+Tl^0(1)$. The data are presented in Fig. 7. In Sec. III D of Ref. 10, it was already argued that both $Tl^0(1)$ and $Tl^+Tl^0(1)$ may be assumed to remain randomly distributed among their possible orientations under the laser excitation.

For randomly oriented point defects, the number of independent intensity parameters (IP) introduced in the BT method reduces to four in the case of RRS. They will be denoted by their shorthand notation,[12]

$$q = 8kI_0N(T_{11}^2 + T_{22}^2 + T_{33}^2) , \tag{1a}$$

$$s = 4kI_0N(T_{12}^2 + T_{21}^2 + T_{31}^2 + T_{13}^2 + T_{23}^2 + T_{32}^2) , \tag{1b}$$

$$r = 8kI_0N(T_{11}T_{22} + T_{22}T_{33} + T_{33}T_{11}) , \tag{1c}$$

$$s' = 8kI_0N(T_{12}T_{21} + T_{13}T_{31} + T_{23}T_{32}) . \tag{1d}$$

k is an instrumental efficiency factor and I_0 is the intensity of the incident beam. The population number N is equal for all the possible orientations of the defect. The elements T_{ij} of the Raman tensor $\overleftrightarrow{T}$ correspond to an arbitrary initial orientation of the defect and are expressed in the reference frame (x,y,z) fixed to the $\langle 100 \rangle$ crystal directions.

It is obvious from (1b) and (1d) that the intensity parameters s and s' are equal for symmetric Raman tensors. The s' IP, which only occurs in the resonant case, is always measured together with the r IP (Ref. 13). This fact is taken into account in the following relations, which associate the experimentally observed intensities $I_{\alpha,\beta}$ measured in the optical geometry 3 (Ref. 12) with the IP. The subscripts α and β indicate the polarization of the incident and scattered light in the reference frame fixed to the $\langle 100 \rangle$ crystal axes:

$$I_{x,yz} = s , \tag{2a}$$

$$I_{y\bar{z},y\bar{z}} = \tfrac{1}{2}[q + (r + s')] + \tfrac{1}{2}s , \tag{2b}$$

$$I_{y\bar{z},yz} = \tfrac{1}{2}[q - (r + s')] + \tfrac{1}{2}s . \tag{2c}$$

It is easy to verify that taking s equal to s', the relations (2) reduce to the well-known relations for nonresonant Raman scattering.

From Fig. 7 the values of q, s, and $r + s'$ can be determined. These values define the observed (RRS) BT of the Raman mode. For the case of RRS on randomly oriented

defects, 13 observed BT's can be distinguished. They are listed in Table II. Within experimental accuracy, the following BT relations are verified for the low-frequency mode of $Tl^+Tl^0(1)$ in RbCl (See Fig. 7):

$$q \neq 0 , \tag{3a}$$

$$\frac{s}{q} = 0.4 \pm 0.1 , \tag{3b}$$

$$\frac{r+s'-s}{q} = -0.1 \pm 0.1 . \tag{3c}$$

It should be emphasized that quantitatively, the relations (3b) and especially (3c) strongly depend on the particular $Tl^+Tl^0(1)$ mode under study and on the excitation frequency. However, we have checked that the polarized Raman data always yield the same BT. The relations (3) allow one to eliminate most of the BT's listed in Table II: The BT's 2, 7, 10, 11, 12, and 13 are not consistent with the relations (3a) and (3b). The relation (3c) yields the ratio r/q under the assumption that s and s' are equal in magnitude: As such, the observation of (3c) is at variance with the IP relations of the BT's 4, 6, and 9. At this point one should consider an additional condition, which follows from the definition of the IP in (1b) and (1d). The polarized Raman data on randomly oriented centers should always obey the relation

$$s \geq |s'| . \tag{4}$$

Assuming that the r IP is equal to either $-\frac{1}{2}q$ or q, corresponding to the BT's 3 and 5, respectively, the experimental BT relations (3) violate the condition (4). As a result, only the BT's 1 and 8 are consistent with the polarized Raman data of the low-frequency resonance of $Tl^+Tl^0(1)$. The representative modes, corresponding to these BT's are repeated below: For BT 1,

$$C_1{:}A,\ C_2[010]{:}A,\ C_2[110]{:}A,\ D_2[110]{:}A . \tag{5a}$$

For BT 8

$$C_4[001]{:}A . \tag{5b}$$

The BT 1 is the one we favor, because it is compatible with a defect symmetry without an inversion center and possessing mirror planes. Through the representative mode $D_2[110]{:}A$ (see Table VI in Ref. 12), BT 1 is entirely consistent with the ODESR analysis, which attributes the $C_{2v}[110]$ symmetry to the $Tl^+Tl^0(1)$ center.[9] However, the BT method does not allow one to discern between the $C_{1h}(010)$ symmetry, corresponding to a $Tl^0(1)$ center which is weakly perturbed by an adjacent Tl^+ ion, and the $C_{2v}[110]$ symmetry indicating a dimer-center structure with two equivalent thallium nuclei. Both these possibilities will be considered in Sec. V.

It is instructive to compare the conclusion of the RRS BT analysis with the result which would be obtained by ordinary BT analysis. Ignoring the fact that s and s'

TABLE II. The behavior types (BT's) are presented, which are distinguishable in the case of RRS on randomly oriented defects. The BT's are defined by the mutual relations between the three intensity parameters (IP's) q, $r+s'$, and s, which can be experimentally determined. The correspondence between the observed BT's and the representative modes is also listed.

BT number[a]	IP relations			Representative modes
1[b]	q	$r+s'$	s	$C_1{:}A$ $C_2[010]{:}A$ $C_2[110]{:}A$
1[b]	q	$r+s$	s	$D_2[110]{:}A$
2	0	s'	s	$C_2[010]{:}B$ $D_2[100]{:}B_1$ $D_2[110]{:}B_2$ $D_2[110]{:}B_3$ $C_4[001]{:}E$ $D_4[001]{:}E$ $T{:}T$
3	q	$-\frac{1}{2}q+s'$	s	$C_2[110]{:}B$ $C_3[111]{:}E$ $D_3[111]{:}E$
4	q	$-\frac{1}{2}q-s$	s	$D_2[110]{:}B_1$
5	q	$q+s'$	s	$C_3[111]{:}A$
6	q	$q+s$	s	$D_3[111]{:}A_1$
7	0	$-s$	s	$D_3[111]{:}A_2$ $D_4[001]{:}A_2$ $O{:}T_1$
8	q	$r-s$	s	$C_4[001]{:}A$
9	q	$-\frac{1}{2}q+s$	s	$C_4[001]{:}B$
10	0	s	s	$D_4[001]{:}B_2$ $O{:}T_2$
11	q	r	0	$D_2[100]{:}A$ $D_4[001]{:}A_1$
12	q	$-\frac{1}{2}q$	0	$D_4[001]{:}B_1$ $T{:}E$ $O{:}E$
13	q	q	0	$T{:}A$ $O{:}A_1$

[a]For convenience of the reader, the 13 BT's for RRS of randomly oriented centers are relabeled; the numbers of Ref. 12 are completely ignored.

[b]The fact that s may be equal to s' cannot be verified, since no relation exists between r and q. As a result these BT's cannot be distinguished.

might be different for RRS, the relations (3) define the observed BT 60 (Table VII in Ref. 12), which is equal to BT 1 in Table II. In contrast, the RRS BT method also allows the representative mode $C_4[001]:A$. Its Raman tensor is purely diagonal for nonresonant Raman scattering, but possesses an antisymmetric contribution in the case of RRS.[17]

Finally, a more simplistic derivation of the irreducible representation of the low-frequency resonance is given, starting from the $C_{2v}[110]$ symmetry, which was attributed to the $Tl^+Tl^0(1)$ center on the basis of the ODESR measurements.[9] In this defect symmetry, only the A_1 mode corresponds to a Raman tensor, possessing both nonzero diagonal and off-diagonal components (see Table V in Ref. 12). As such only the A_1 mode of $C_{2v}[110]$ is compatible with (3a) and (3b). Its Raman tensor, expressed in the crystal reference frame reads as follows:

$$C_{2v}[110]:A_1 \begin{bmatrix} a & -c & 0 \\ -c' & a & 0 \\ 0 & 0 & a_3 \end{bmatrix} . \tag{6}$$

It is obvious that this simple argument is valid, whether or not nonsymmetric Raman tensors are considered. However, it does not possess the inductive character of the BT approach.

V. DISCUSSION

A. Resonant enhancement of the Raman scattering

The C_{4v} symmetry derived from the Raman data under OT3 excitation is compatible with both the $C_{2v}[110]$ and the $C_{1h}(010)$ defect symmetries, derived from the RRS BT analysis of the Raman data obtained under OT4 excitation. Under excitation of OT3 of $Tl^+Tl^0(1)$, the resonance condition obscures the lower symmetry of the dimer center, through the *selective resonant enhancement* of one of the diagonal components of the Raman tensor (see Table V in Ref. 12). As a result, the two other diagonal components and also the off-diagonal components become relatively negligible and an apparent C_{4v} symmetry is observed. This is a typical example of the fact that the observed BT may indicate a higher symmetry than the actual defect symmetry, as was discussed in Sec. II E of Ref. 12.

It must be emphasized that the diagonal component of the Raman tensor, which is resonantly enhanced, corresponds to the direction *perpendicular* to the defect plane in the case of $C_{2v}[110]$ symmetry and to a thallium-vacancy axis (*within* the defect plane) in the case of the $C_{1h}(010)$ point group (see Table V in Ref. 12).

B. Weakly perturbed $Tl^0(1)$ center

The BT method yields two equally possible symmetries for $Tl^+Tl^0(1)$, i.e., $C_{1h}(010)$ and $C_{2v}[110]$. The latter symmetry was derived from magnetic resonance experiments and can be considered to result from averaging of the ESR spectrum by a tunneling motion between two $Tl^0(1)$-like configurations. The $C_{1h}(010)$ point group would then be the instantaneous symmetry and could be observed with the visible light probe (frequency 10^{15} Hz) if the scattering process is sufficiently fast.

In that case, however, one would expect to see a low-frequency vibration of the Tl^0 atom, which was characteristic for the $Tl^0(1)$ defect. The absence of this mode (see Figs. 2—4) and the very different structure of the induced first-order spectrum (compare Fig. 3 with Fig. 2 in Ref. 10) indicate that the picture of a weakly perturbed $Tl^0(1)$ center is not a very appropriate one for $Tl^+Tl^0(1)$.

C. Electron tunneling and the dimer-center structure

The $C_{2v}[110]$ symmetry corresponds to an electronic configuration with two equivalent thallium nuclei, as was established for the ground state of $Tl^+Tl^0(1)$ by ODESR.[9] In order to explain the polarized Raman data under OT3 excitation one can consider a tunneling model in the limit of extreme localization in which the electronic structure of the dimer center is described by linear combinations of the unperturbed $Tl^0(1)$-like wave functions. In this approach the OT3 of $Tl^+Tl^0(1)$ connects the ground-state tunnel doublet $\psi_0^{\pm}$,

$$\psi_0^{\pm} = \frac{1}{\sqrt{2}}(\phi_0^1 \pm \phi_0^2) , \tag{7a}$$

with the excited-state doublet $\psi_e^{\pm}$,

$$\psi_e^{\pm} = \frac{1}{\sqrt{2}}(\phi_e^1 \pm \phi_e^2) . \tag{7b}$$

ϕ_0^i and ϕ_e^i indicate the Φ ground-state wave function and the Σ excited state of the ith $Tl^0(1)$ center, respectively.[7] The even and odd combinations in (7) transform according to the A_1 and B_1 representations of $C_{2v}[110]$, respectively. Taking into account that the Raman scattering cross section under OT3 excitation is proportional to

$$\langle \psi_0^{\pm} | \bar{r} | \psi_e^{\pm} \rangle \langle \psi_e^{\pm} | \bar{r} | \psi_0^{\pm} \rangle , \tag{8}$$

the following vibrations can be resonantly enhanced under OT3 excitation:

$$(A_1 + B_1) \otimes (A_1 + B_1) = 2A_1 + 2B_1 . \tag{9}$$

As such the tunneling model is consistent with the resonant enhancement of the A_1 modes. However, it does not explain precisely why the a_3 component of (6) is resonantly enhanced under OT3 excitation. This component is associated with a modulation of the polarizability *perpendicular* to the $Tl^+Tl^0(1)$ defect plane. Its resonant enhancement must be related to the different electronic structure of $Tl^+Tl^0(1)$ compared to $Tl^0(1)$, the low symmetry of which allows a more complicated mixing of electronic wave functions, in comparison with the $Tl^0(1)$ center. This problem requires additional MCD experiments in order to be clarified.

D. Observability of the electron tunnel splitting

An interesting question concerns the observability in the Raman spectrum of the electronic ground-state tunnel splitting (resonance splitting) of the $Tl^+Tl^0(1)$ center. According to (7a), this transition is Raman active, since it belongs to the B_1 representation of $C_{2v}[110]$. As such, it

is not directly observed, because all the Raman modes both under OT3 and OT4 excitation exclusively belong to the totally symmetric A_1 representation. At this point two alternative interpretations of these A_1 Raman modes can be put forward.

First, the Raman modes may be "*pure*" phonon modes, which transform according to the A_1 representation of $C_{2v}[110]$. Such modes do not affect the equivalence between the two potential wells of the static electronic potential, and consequently they do not assist in the electron tunneling.

Second, the electron resonance splitting may be detected through *sidebands* of phonons belonging to the B_1 representation, which are superimposed on the tunnel transitions. Under the assumption of a linear coupling between the phonons and the tunneling, these sidebands transform according to the product of the representation of the B_1 phonons and the tunnel transition, which is indeed the A_1 representation. The B_1 modes certainly assist in the electron tunneling. In particular, in the low-frequency B_1 modes one thallium nucleus moves towards the anion vacancy, while the other moves away from it, and this asymmetric modulation of the electronic potential forces the unpaired electron to tunnel from one thallium ion to the other.

VI. CONCLUDING REMARKS

The dynamical and electronic properties of the Tl^+-perturbed $Tl^0(1)$ center have been investigated by polarized resonant Raman scattering. The Raman data obtained under excitation of the third optical band of $Tl^+Tl^0(1)$ were analyzed by the behavior-type method, and a totally symmetric defect-induced first-order spectrum in a C_{4v} symmetry was established. The spectra measured under excitation of the fourth optical band were analyzed by means of the extended behavior-type method for resonant Raman scattering. This analysis reveals the lower symmetry of $Tl^+Tl^0(1)$. The representative symmetry was determined to be $D_2[110]$, leaving essentially two possibilities for the actual defect symmetry as observed by Raman scattering. It is either $C_{1h}(010)$, corresponding to a weakly perturbed $Tl^0(1)$-like configuration, or $C_{2v}[110]$, to be associated with electron tunneling between the two thallium nuclei. One could discern between these two alternatives, if more detailed knowledge about the optical properties of the third transition of $Tl^+Tl^0(1)$ was available.

ACKNOWLEDGMENTS

The authors are indebted to M. Leblans for clarifying discussions about the extension of the behavior-type method for the case of resonant Raman scattering. Helpful discussions with F. Ahlers, F. Lohse, and J. M. Spaeth and expert experimental assistance of A. Bouwen are kindly acknowledged. This work was supported by the Geconcerteerde Acties, the Interuniversitair Instituut voor Kernwetenschappen (IIKW), and the National Fund for Scientific Research (NFWO).

[1]L. F. Mollenauer, in *The Laser Handbook,* edited by M. L. Stitch and M. Bass (North-Holland, Amsterdam, 1985), Vol. 4, Chap. 2.

[2]E. Goovaerts, J. Andriessen, S. V. Nistor, and D. Schoemaker, Phys. Rev. B **24**, 29 (1981).

[3]P. G. Baranov and V. A. Kramtsov, Phys. Status Solidi B **101**, 153 (1980).

[4]W. Gellermann, F. Lüty, and C. R. Pollock, Opt. Commun. **39**, 391 (1981); International Conference on Defects in Insulating Crystals, Salt Lake City, 1984 (unpublished), p. 171.

[5]L. F. Mollenauer, N. D. Viera, and L. Szeto, Opt. Lett. **9**, 414 (1982).

[6]I. Heynderickx, E. Goovaerts, S. V. Nistor, and D. Schoemaker, Phys. Status Solidi B **135**, 69 (1986).

[7]L. F. Mollenauer, N. D. Viera, and L. Szeto, Phys. Rev. B **27**, 5332 (1983).

[8]F. J. Ahlers, F. Lohse, J. M. Spaeth, and L. F. Mollenauer, Phys. Rev. B **28**, 1249 (1983).

[9]F. J. Ahlers, F. Lohse, and J. M. Spaeth, J. Phys. C **18**, 3881 (1985).

[10]W. Joosen, E. Goovaerts, and D. Schoemaker, J. Lumin. **31-32**, 317 (1984), Phys. Rev. B **32**, 6748 (1985).

[11]W. Gellermann, T. Jock, and F. Lüty, International Conference on Defects in Insulating Crystals, Salt Lake City, 1984 (unpublished), p. 167.

[12]J. F. Zhou, E. Goovaerts, and D. Schoemaker, Phys. Rev. B **29**, 5509 (1984); E. Goovaerts, J. F. Zhou, W. Joosen, and D. Schoemaker, Cryst. Latt. Defects Amorph. Mater. **12**, 317 (1985).

[13]M. Leblans, W. Joosen, E. Goovaerts, and D. Schoemaker, Phys. Rev. B **35**, 2405 (1987).

[14]J. F. Zhou, E. Goovaerts, and D. Schoemaker, Phys. Rev. B **29**, 5533 (1984).

[15]W. Joosen, J. F. Zhou, E. Goovaerts, and D. Schoemaker, Phys. Rev. B **31**, 6709 (1985).

[16]W. Joosen, E. Goovaerts, and D. Schoemaker, Phys. Rev. B **34**, 1273 (1986).

[17]L. N. Ovander, Opt. Spectrosc. **9**, 302 (1960).